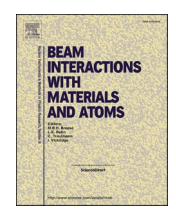
FISEVIER

Contents lists available at ScienceDirect

# Nuclear Inst. and Methods in Physics Research, B

journal homepage: www.elsevier.com/locate/nimb





# External beam normalization measurements using atmospheric argon gamma rays

John T. Wilkinson\*, Sean R. McGuinness, Graham F. Peaslee

Department of Physics, University of Notre Dame, Notre Dame, IN 46556, USA

ARTICLE INFO

Keywords:
PIGE
External beam
Beam current integration
Argon normalization

#### ABSTRACT

Particle-induced gamma-ray emission spectroscopy is a quantitative, sensitive technique that measures light element abundance in materials using external reference standards with known beam energy and intensity. When the ion beam is used *ex vacuo*, gamma-ray spectroscopy on targets in air greatly increases sample throughput. However, for most targets the accuracy of these measurements is limited by the uncertainty of the collected charge. An indirect beam current measurement technique has been developed using an ion beam reaction on atmospheric argon, the only atmospheric component with sufficient abundance ( $\sim$ 1%) that produces abundant gamma rays with low-energy proton beams. The  $^{40}$ Ar(p,n $\gamma$ ) $^{40}$ K reaction has been studied here, and the characteristic 770 keV gamma ray is observed to serve as a reliable monitor for proton flux. This method allows a real-time calibration of beam intensity on target to measured upstream currents for ion beam analysis at beam energies above 3.5 MeV.

## 1. Introduction

The use of external ion beams has grown significantly in recent years for a variety of ion beam analysis applications [1–3]. This *ex-vacuo* technique can offer expedited analysis while avoiding vacuum considerations on sensitive samples [4–6]. High reaction cross sections allow for quick identification of some elements and isotopes at low bombarding energies of a few MeV [7]. Particle-induced gamma-ray emission (PIGE) and particle-induced x-ray emission (PIXE) are two such examples of ion beam analysis easily performed in atmosphere. PIGE involves the inelastic scattering of MeV range protons to excite the target nuclei. The de-excitation of target nuclei yields an isotopic signature for identification [8], which allows for a quick spectroscopic survey of targets and isotopic identification of materials present. The higher-energy gamma rays produced by PIGE are observed with little atmospheric interference, unlike many of the low-energy x-rays produced by PIXE.

Still, the challenge of measuring an accurate beam intensity on target has detracted from the accuracy of these methods. Shielded and suppressed Faraday cups can give accurate beam intensity measurements before and/or after a sample measurement, but then the beam stability over the sample analysis time must be estimated. In addition, extraction of ions into atmosphere can introduce straggling and degrade the energy

and angular resolution of the beam. In many scenarios, an absolute yield is difficult to determine to better than 10%, but by assuming beam stability and by making many measurement comparisons of known standards, relatively accurate concentrations are possible. Other beam intensity measurements for external ion beams have been achieved in various ways including normalizing beam intensity off gamma rays from an exit foil, backscattered protons, x-rays from a rotating chopper, and argon x-rays [9–12]. However, external foils must be carefully chosen not to degrade with time and not to interfere with the measurement of target materials, in addition to estimating their effect on beam energy and divergence. Similarly, measuring the low-energy (2.96 KeV) Ar x-rays in air requires both a thin-window x-ray detector and an estimation of the detection efficiency through the air gap.

For example, one case where none of these methods were particularly useful in reducing beam intensity uncertainties was the use of ion beam analysis as a viable screening technique for environmental toxins, and a rapid analysis of targets that has been established for this purpose *ex vacuo* [13–16]. Accurate analysis of samples and standards requires precision monitoring of beam currents during the live run window, but a simultaneous charge integration is not always possible due to the wide array of non-conducting thin and thick targets measured [17–19].

For gamma spectroscopy using proton energies greater than 3.5 MeV, an alternative fusion-evaporation reaction –  $^{40}\text{Ar}(p,n\gamma)^{40}\text{K}$  – is

E-mail address: jwilkin5@nd.edu (J.T. Wilkinson).

 $<sup>^{\</sup>ast}$  Corresponding author.

proposed as an indirect measurement of beam flux. Gamma-ray producing reactions on atmospheric  $^{40}$ Ar deliver a more precise yield than x-rays and do not require additional equipment for PIGE measurements. The abundance of argon in the atmosphere (about 1%) offers a monitor that scales well with beam intensity and does not interfere with typically observed lines [7]. The simultaneously observed (p,n $\gamma$ ) reaction on atmospheric argon allows for rapid testing of all target matrices while maintaining precise measurement of delivered beam for PIGE analysis.

#### 2. Methods

The  $^{40}\text{Ar}(p,n\gamma)^{40}\text{K}$  reaction was studied at the University of Notre Dame's Nuclear Science Laboratory (NSL) using the St. Andre ion beam analysis facility [16]. Simultaneous external PIGE and PIXE measurements at the NSL typically involve 3-minute irradiations with intensities of 30–60 nA at 4 MeV. In this experiment, most of the measurements were made at 4.2 MeV, but bombarding energies between 3.4 and 5.2 MeV were also used.

The proton beam was tuned to pass through a 3/8'' (9.525 mm) diameter tantalum collimator and exit into atmosphere through an  $8-\mu m$  Kapton® foil. This foil is replaced routinely after 24 h of use at these beam energies to minimize foil degradation and thickening [20]. Typical targets for analysis by PIGE spectroscopy are mounted at a fixed 30 mm distance from the exit port, and a Canberra® high-purity-germanium detector is fixed at  $45^\circ$  to the beam at 30 mm beyond the target position. An optional silicon drift detector is also positioned at approximately  $135^\circ$  to the beam and above the beam-target assembly.

Beam delivery to target consisted of visual confirmation of beam focus using a glass scintillator at the target position, as well as minimization of current readings on upstream apertures. For each irradiation, the beam was first measured by an integrated current measurement on an upstream suppressed Faraday cup for ten seconds, another ten seconds on the aperture, and finally on an electrically isolated thick tantalum foil placed at the target position for the duration of the run. The thick target is necessary to completely stop the protons, ensuring that for each run, the beam is exposed to the same amount of atmosphere (the same length of travel). Upon completion, the cup and aperture current readings were integrated for another ten seconds each, in reverse order. The integrated charge delivered to target, as measured upstream, was varied from 6 to 54  $\mu$ C, far exceeding typical running parameters of 6-12 µC. Three beam currents (36, 50 and 90 nA), and three analysis times (3, 5 and 10 min), comprised this range. These absolute charge measurements served as a scale to measure transmission from internal Faraday cup to target ex vacuo. The excitation curve was also mapped for the atmospheric thick target for beam energies between 3.4 and 5.2 MeV. For the most statistics, the excitation yield was measured for ten minutes at currents greater than 100 nA with periodic checks done at lower currents (~20 nA).

The  $^{40} Ar(p,n\gamma)^{40} K$  reaction was measured via the cascade of the 800 keV second excited state to the ground state in  $^{40} K$  [21]. The emission of both 29 keV and 770 keV gamma rays were observed on the silicon drift and high-purity germanium detectors, respectively. While the 29 keV gamma-ray was also observed in the high-purity germanium detector, the high background observed below 100 keV disqualified its use as a normalization line. The 770 keV transition was chosen as the normalization peak for its low background, minimal neighboring peaks, and increased yield from higher energy gamma-ray cascades observed at higher bombarding energies. A sample spectrum is shown in Fig. 1.

#### 3. Results

# 3.1. External beam normalization

Changes in beam intensity, either intentional or due to tune degradation, can lead to discrepancies between Faraday cup currents and the actual beam delivered to target. The normalization survey was first

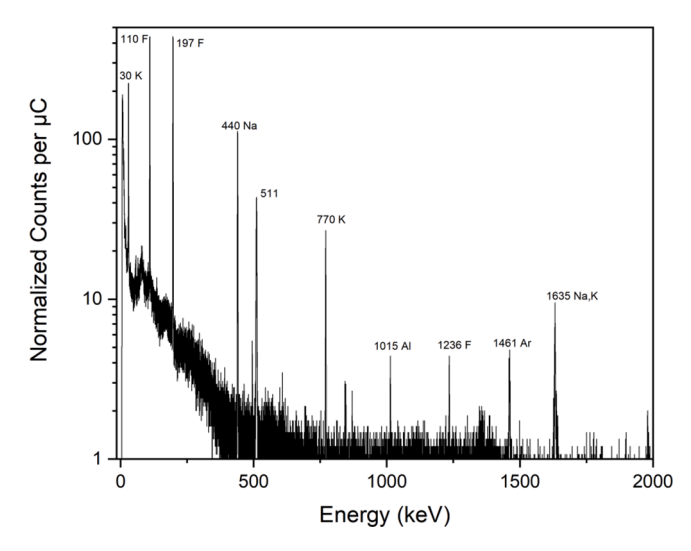


**Fig. 1.** The spectrum is a sample of the sodium fluoride standard reference material observed at a 4.0 MeV bombarding energy. The listed gamma-ray energies are in keV with their respective source. The prominence of the 770 keV line is clear. Note the above elements are monoisotopic except for argon and potassium. The argon and potassium isotopes are both mass 40, with potassium being derived from the exchange reaction on atmospheric argon.

performed at a fixed beam energy (4.0 MeV), varying only the beam intensity and irradiation time. For the fixed geometry previously described, this method explored the use of argon as an internal standard to all spectra, acting as an indirect normalization during the data acquisition. This first investigation sought to determine if transmission was current dependent. After charge delivery was studied extensively, the beam energy was varied. In this experiment, upstream Faraday cup current measurements were proportional to delivered current, but fractional beam losses through collimators, magnets, and air lead to a different transmission factor for a different beam energy and subsequent set of beam parameters. Apart from steering the beam off target, the observed yield scales with the ex vacuo current. Normalization using just the upstream current results in over-normalized delivered charge (i.e. a too high charge on target), with respect to the beam intensity measurements made by the <sup>40</sup>Ar external monitoring method. The changes in transmission are not always quantifiable but are internally accounted for by measuring yield changes. Use of the Faraday cup current alone introduces systematic errors by normalizing to a delivered charge only achievable with perfect transmission to target. The indirect measurement of proton interaction with atmosphere is therefore better at measuring target current than any upstream Faraday cup estimates as it serves to scale with transmission. The 30 mm atmospheric thick target is used to normalize to the true beam intensity measured upstream. In practice, this means that the yield of 770 keV gamma rays measured per μC of beam delivered serves as the normalization signal for all other observed gamma rays during the irradiation.

The result of this charge varied yield is shown in Fig. 2, which is an effective model for transmission. The charge delivered to target scaled directly with analysis time, but the charge delivered to target was reduced at higher beam intensity.

This inverse relationship between the beam intensity measured in the upstream Faraday cup compared to the atmospheric yield of  $^{40}\mbox{Ar}$  gamma rays/ $\mu\mbox{C}$  represents a loss of transmission from Faraday cup to final impingement on the target. The beam's areal intensity is not uniform and does not scale symmetrically for a given set of beam parameters. Fractional losses through the magnets and apertures is more evidence supporting the need for an external normalization close to the sample.

As an example of how beneficial this technique may become to typical ion beam analysis *ex vacuo*, Table 1 shows the decreased error

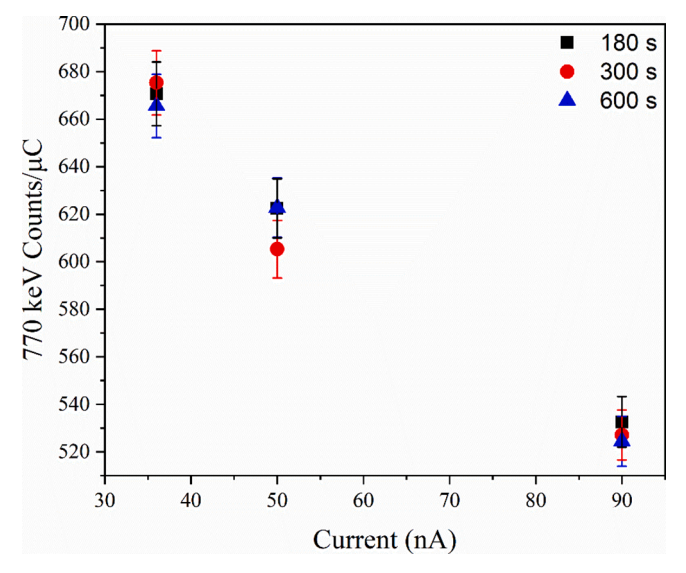


**Fig. 2.** Effective yield of atmospheric argon interaction shows a loss of transmission into atmosphere as beam current is increased at 4.0 MeV. Consistent transmission would expect a horizontal trend in yield.

$$\label{eq:control_equation} \begin{split} & \textbf{Table 1} \\ & \text{Duplicate standard ratios, } N = 57. \end{split}$$

Faraday cup normalized ratio	Faraday Cup normalized standard Deviation	Argon normalized Ratio	Argon normalized Standard Deviation
1.012	0.213	0.997	0.083

obtained in duplicate standard reference materials analyzed hours apart over several days. The tabulated ratio consists of repeated measurements of five different sodium fluoride target concentrations analyzed for proof of principle. The investigated gamma rays were the 109 and 197 keV excitations of fluorine. While Faraday cup normalization can be as accurate, normalization with respect to atmospheric argon is more precise, reducing the relative standard deviation from 21% to 8%. This was verified with an f-test,  $F_{1,56}=0.153$  and p<0.0001, proving the reduction in variance for the argon normalized data. Similarly, since these are the same standards, the accuracy improved from 1.2% to 0.3% by normalizing to the beam intensity using the  $^{40}\text{Ar}(p,n\gamma)^{40}\text{K}$  reaction. Only standards processed hours apart were included in Table 1 and so N is not an even multiple of the five standards.

### 3.2. Energy selection

Charge integration on the thick tantalum foil allowed for a transmission coefficient to be calculated for a normalized Ar gamma-ray yield (counts/ $\mu$ C). All apertures downstream of the Faraday cup were monitored for every energy. The apertures and tantalum target foil were unsuppressed current measurements. Average transmission to target (at the 30 mm foil position) was 87% but varied between 71% and 93%. The 770 keV gamma rays emitted from the de-excitation of the second to the first excited state of  $^{40}$ K is the primary line of interest. The transmission corrected yield as a function of bombarding energy is shown in Table 2.

Table 2 consists of a listing of nominal beam energies in vacuum, SRIM modeled energy after the 8  $\mu m$  Kapton® exit foil, SRIM modeled energy after the consistent 30 mm air gap, and the normalized yield [22]. These data are plotted in Fig. 3 where the given energies are that in vacuum. The yield is transmission corrected for every energy. The determined transmission values were done with currents ranging from 20 nA to 200 nA. No correlation was noted between transmission and upstream Faraday cup currents.

**Table 2**Tabular data of normalized 770 keV yield.

Energy (keV)	After kapton	After Air	Normalized yield (Counts/μC)
3400	3290	2945	$3\pm0.3$
3425	3316	2971	$10\pm0.4$
3450	3342	2997	$17\pm0.5$
3475	3367	3023	$26\pm0.7$
3500	3393	3048	$39 \pm 0.9$
3525	3418	3074	$45\pm1.1$
3550	3444	3099	$54\pm1.3$
3575	3470	3124	$71 \pm 1.6$
3600	3495	3149	$124\pm2.5$
3625	3521	3174	$174 \pm 3.5$
3650	3546	3199	$212\pm4.2$
3675	3572	3224	$231 \pm 4.5$
3700	3598	3249	$218\pm2.7$
3725	3623	3273	$219 \pm 4.2$
3750	3649	3298	$240 \pm 4.5$
3775	3674	3322	$261 \pm 4.9$
3800	3700	3346	$289 \pm 3.7$
4200	4107	3728	$443 \pm 4.6$
4600	4512	4104	$587 \pm 5.7$
4800	4714	4292	$839 \pm 14.8$
5000	4917	4481	$884 \pm 7.2$
5100	5018	4577	$910\pm14.9$
5200	5118	4674	$1036\pm21.9$

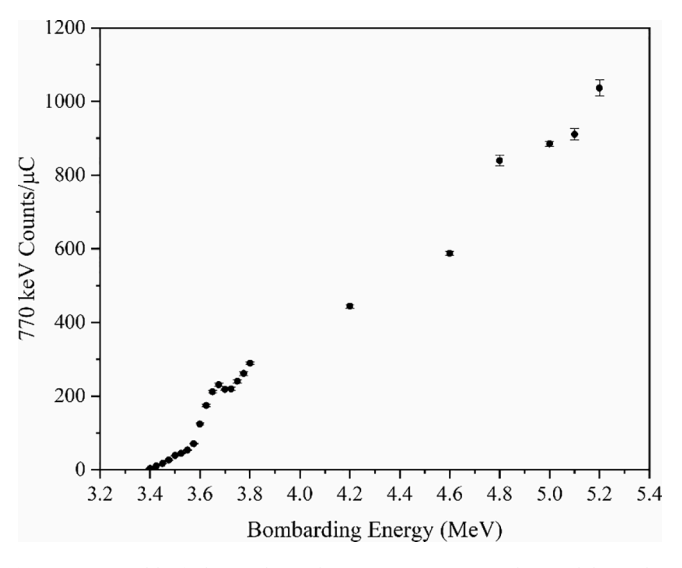


**Fig. 3.** Raw yield of observed 770 keV gamma rays per charge delivered as determined by transmission-corrected Faraday cup currents. Some uncertainties are smaller than the data marker. The upstream currents were used for the proof of principle for downstream yields and not as an absolute calibration. The trend of the yield agrees with differential cross sections previously published although this is an integrated thick target yield [21].

As shown in Fig. 3, energy mapping ranged from 3.4 to 5.2 MeV. The lower energy of this domain approaches zero and therefore this method ceases to be useful as a precise monitor for beam current fluctuations. The (p,n) reaction threshold is at (E<sub>lab</sub> = 2.345 MeV), but the first excited state's 29 keV gamma-ray was rejected for wide background fluctuations across this energy range [21]. As this method is sought to accurately monitor changes in beam intensity on target, much of the low bombarding energy work serves only as a baseline for yield statistics. The upper limit was established due to detector rate limits, caused by activation of atmosphere resulting in  $^{14}\mathrm{O}$ , short-lived positron emitters with no other gammas, and gamma-rays from the scattering of the  $^{14}\mathrm{N}$  (p,py) $^{14}\mathrm{N}$  and  $^{15}\mathrm{N}$  (p,py) $^{15}\mathrm{N}$  reactions [23].

#### 4. Conclusion

Use of this method has significantly decreased systematic errors (by approximately a factor of two) for comparative external PIGE measurements at the NSL. All tuning parameters are optimized for initial transmission to target, and several stable Faraday cup current measurements (before and after an irradiation) are the inputs for the calibration normalization. As the beam fluctuates throughout the day, this <sup>40</sup>Ar(p,nγ)<sup>40</sup>K reaction monitors beam delivery to target. The spectroscopic analysis then normalizes the yield of the observed gamma-ray(s) of interest to the integrated 770 keV gamma-ray yield. Unobserved beam dips or spikes during the live run-time are now accounted for, which allows better reproduction of standard reference material results. Standard reference materials run at different times better reproduce initial vields because of this normalization. While absolute vields vary. normalized yields are comparable to within uncertainties, of which the leading errors stem from the targets themselves. This methodology serves only to act as an indirect measurement and does not determine an absolute external proton fluence without the use of external standard targets.

Precision monitoring at the NSL has optimized analysis parameters of any fixed energy between 3.8 and 4.8 MeV with 5–15  $\mu C$  delivered charge to avoid sample damage. It has also been observed that thin target yields are decreased due to an inflated argon normalization coming from argon excitation continuing after passing through the target. This occurrence is easily remedied by backing the targets with paper or plastic, however, so the beam falls below the threshold energy if it continues into atmosphere. While this monitoring reaction is highly correlated with argon x-rays, secondary fluorescence of gamma-rays is not a concern and the sensitivity of the low-energy x-rays to the air gap is avoided as well. The 770 keV gamma-ray normalization benefits PIGE and simultaneous PIXE ex-vacuo.

#### CRediT authorship contribution statement

John T. Wilkinson: Conceptualization, Methodology, Validation, Formal analysis, Investigation, Writing - original draft, Writing - review & editing, Visualization. Sean R. McGuinness: Conceptualization, Methodology, Software, Investigation, Writing - review & editing. Graham F. Peaslee: Conceptualization, Writing - review & editing, Supervision, Project administration, Funding acquisition.

#### **Declaration of Competing Interest**

The authors declare that they have no known competing financial interests or personal relationships that could have appeared to influence the work reported in this paper.

# Acknowledgements

This work was supported by the U.S. Department of Defense Strategic Environmental Research and Development Program [grant number ER19-1142]; the National Science Foundation [grant number PHY-1713857]. We would also like to thank Edward Stech, Daniel Robertson, Brian Huge, and Haley Borsodi for their assistance throughout the project. This work was conducted at the Nuclear Science Laboratory at the University of Notre Dame.

#### References

- [1] P.S. Dhorge, P.S. Girkar, A.D. Sharma, T. Keesari, N.S. Rajurkar, R. Acharya, P. K. Pujari, Application of in situ current normalized Particle Induced Gamma-ray Emission (PIGE) method for determination of total fluorine concentration in sediment samples from different geological provinces and its relevance to fluoride contamination, Geochemistry (2019) 125551, https://doi.org/10.1016/j.chemer.2019.125551.
- [2] G.S. Hall, E. Navon, Proton-induced X-ray and gamma ray emission analysis of biological samples, Nucl. Instrum. Methods Phys. Res. Sect. B Beam Interact. Mater. Atoms 15 (1-6) (1986) 629–631.
- [3] R. Huszank, L. Csedreki, Z. Török, Direct trace element analysis of liquid blood samples by in-air ion beam analytical techniques (PIXE-PIGE), Anal. Chem. 89 (3) (2017) 1558–1564.
- [4] M. Vadrucci, G. Bazzano, F. Borgognoni, M. Chiari, A. Mazzinghi, L. Picardi, C. Ronsivalle, C. Ruberto, F. Taccetti, A new small-footprint external-beam PIXE facility for cultural heritage applications using pulsed proton beams, Nucl. Instrum. Methods Phys. Res. Sect. B Beam Interact. Mater. Atoms 406 (2017) 314–317.
- [5] I. Reiche, C. Heckel, K. Müller, O. Jöris, T. Matthies, N.J. Conard, H. Floss, R. White, Combined non-invasive PIXE/PIGE analyses of mammoth ivory from aurignacian archaeological sites, Angew. Chem. Int. Ed. 57 (25) (2018) 7428–7432.
- [6] Á.Z. Kiss, E. Koltay, B. Nyakó, E. Somorjai, A. Anttila, J. Räisänen, Measurements of relative thick target yields for PIGE analysis on light elements in the proton energy interval 2.4–4.2 MeV. J. Radioanal. Nucl. Chem. Articles 89 (1) (1985) 123–141.
- [7] M.J. Kenny, J.R. Bird, E. Clayton, Proton induced γ-ray yields, Nucl. Instrum. Methods 168 (1-3) (1980) 115–120.
- [8] J. Räisänen, A rapid method for carbon and oxygen determination with external beam proton induced gamma-ray emission analysis, Nucl. Instrum. Methods Phys. Res. Sect. B Beam Interact. Mater. Atoms 17 (4) (1986) 344–348.
- [9] Y.a. Xu, M.i. Xu, G.-F. Wang, C.-L. Zheng, M.-L. Qiu, Y.-J. Chu, Beam charge integration in external beam PIXE–PIGE analysis utilizing proton backscattering with an extraction window, Nucl. Sci. Technol. 27 (6) (2016), https://doi.org/ 10.1007/s41365-016-0131-5.
- [10] M. Chiari, A. Migliori, P.A. Mandò, Measurement of low currents in an external beam set-up, Nucl. Instrum. Methods Phys. Res. Sect. B Beam Interact. Mater. Atoms 188 (1-4) (2002) 162–165.
- [11] Ž. Šmit, M. Uršič, P. Pelicon, T. Trček-Pečak, B. Šeme, A. Smrekar, I. Langus, I. Nemec, K. Kavkler, Concentration profiles in paint layers studied by differential PIXE, Nucl. Instrum. Methods Phys. Res. Sect. B Beam Interact. Mater. Atoms 266 (9) (2008) 2047–2059.
- [12] L. Schultes, G.F. Peaslee, J.D. Brockman, A. Majumdar, S.R. McGuinness, J. T. Wilkinson, O. Sandblom, R.A. Ngwenyama, J.P. Benskin, Total fluorine measurements in food packaging: how do current methods perform? Environ. Sci. Technol. Lett. 6 (2) (2019) 73–78.
- [13] E.E. Ritter, M.E. Dickinson, J.P. Harron, D.M. Lunderberg, P.A. DeYoung, A. E. Robel, J.A. Field, G.F. Peaslee, PIGE as a screening tool for Per- and polyfluorinated substances in papers and textiles, Nucl. Instrum. Methods Phys. Res. Sect. B Beam Interact. Mater. Atoms 407 (2017) 47–54.
- [14] A.E. Robel, K. Marshall, M. Dickinson, D. Lunderberg, C. Butt, G. Peaslee, H. M. Stapleton, J.A. Field, Closing the mass balance on fluorine on papers and textiles, Environ. Sci. Technol. 51 (16) (2017) 9022–9032.
- [15] S. R. McGuinness, J. T. Wilkinson, M. E. Tighe, A. Majumdar, B. Mulder, E. Stech, D. Robertson, G. F. Peaslee. (2019, October). Development of the St. Andre ion beam analysis facility at notre dame. In AIP Conference Proceedings (Vol. 2160, No. 1, p. 050025). AIP Publishing LLC.
- [16] L. Asking, E. Swietlicki, M. Lal Garg, PIGE analysis of sodium in thin aerosol samples, Nucl. Instrum. Methods Phys. Res. Sect. B Beam Interact. Mater. Atoms 22 (1-3) (1987) 368–371.
- [17] A. Re, D. Angelici, A. Lo Giudice, J. Corsi, S. Allegretti, A.F. Biondi, G. Gariani, S. Calusi, N. Gelli, L. Giuntini, M. Massi, F. Taccetti, L. La Torre, V. Rigato, G. Pratesi, Ion beam analysis for the provenance attribution of lapis lazuli used in glyptic art: the case of the "Collezione Medicea", Nucl. Instrum. Methods Phys. Res. Sect. B Beam Interact. Mater. Atoms. 348 (2015) 278–284.
- [18] C. Boni, A. Caridi, E. Cereda, G.M. Braga Marcazzan, P. Redaelli, Simultaneous PIXE-PIGE analysis of thin and thick samples, Nucl. Instrum. Methods Phys. Res. Sect. B Beam Interact. Mater. Atoms. 49 (1-4) (1990) 106–110.
- [19] L. Giuntini, P.A. Mandò, External beam RBS in an unenclosed helium environment, Nucl. Instrum. Methods Phys. Res. Sect. B Beam Interact. Mater. Atoms. 85 (1-4) (1994) 744–748.
- [20] T.M. Young, J.D. Brandenberger, F. Gabbard, Ar 40 (p, n) K 40 reaction from threshold to 5.0 MeV, Phys. Rev. 172 (4) (1968) 1148.
- [21] J.F. Ziegler, M.D. Ziegler, J.P. Biersack, SRIM The stopping and range of ions in matter (2010), Nucl. Instrum. Methods Phys. Res. Sect. B Beam Interact. Mater. Atoms. 268 (11-12) (2010) 1818–1823.
- [22] J.K. Bair, H.O. Cohn, J.D. Kington, H.B. Willard, Reaction N 14 (p, p'  $\gamma$ ) N 14, Phys. Rev. 104 (6) (1956) 1595.